American Journal of Pathology, Vol. 160, No. 6, June 2002

An Invasion-Independent Pathway of Blood-Borne Metastasis

A New Murine Mammary Tumor Model

Takashi Sugino,* Takashi Kusakabe,* Nobuo Hoshi,* Tomiko Yamaguchi,* Takanori Kawaguchi,* Steve Goodison,† Masayuki Sekimata,‡ Yoshimi Homma,‡ and Toshimitsu Suzuki*

From the Departments of Pathology and Biomolecular Science,‡ School of Medicine, Fukushima Medical University, Fukushima City, Japan; and the University of California San Diego Cancer Center and the Department of Pathology,† University of California San Diego, La Jolla, California*

It is generally believed that active invasion by cancer cells is essential to the metastatic process. In this report, we describe a murine mammary tumor (MCH66) model of metastasis that does not require invasion into the vascular wall of both the primary tumor and the target organ, in this case, the lung. The process involves intravasation of tumor nests surrounded by sinusoidal blood vessels, followed by intravascular tumor growth in the lung, without penetration of the vascular wall during the process. Comparative studies using a nonmetastatic MCH66 clone (MCH66C8) and another highly invasive metastatic cell line (MCH416) suggested that high angiogenic activity and sinusoidal remodeling of tumor blood vessels were prerequisites for MCH66 metastasis. Differential cDNA analysis identified several genes that were overexpressed by MCH66, including genes for the angiogenesis factor pleiotrophin, and extracellular matrix-associated molecules that may modulate the microenvironment toward neovascularization. Our analyses suggest that tumor angiogenesis plays a role in the induction of invasion-independent metastasis. This model should prove useful in screening and development of new therapeutic agents for cancer metastasis. ***(Am J Pathol 2002, 160:1973–1980)***

Blood-borne metastasis is a complex biological process comprised of multiple steps, such as intravasation, transport via the blood, extravasation, and secondary growth in the target organ. The invasive property of cancer cells is generally believed to be the most essential factor in this process, and enabling the metastatic cells to break through the vascular wall barrier at the site of dissemination. However, we have previously described an alternative metastatic pathway that does not seem to require invasiveness to the vascular wall in spontaneous mammary tumors.[1] In this metastatic process, tumor nests were enveloped by vascular endothelial cells and entered the circulation, and subsequently, trapped tumor emboli grew within pulmonary arterioles. In this spontaneous mammary tumor model, the metastatic cells do not need to penetrate the vascular wall at either the primary or metastatic tumor site, disseminating via a metastatic pathway that is independent of tumor cell invasiveness. In the absence of invasion, the facilitation of this metastatic process likely requires angiogenesis to envelop tumor emboli with endothelial cells.

To further investigate the mechanisms of invasion-independent metastasis, we established two metastatic cell lines, one highly invasive (MCH416), and one with poor invasive ability (MCH66) from spontaneous mammary tumors. We also derived a nonmetastatic clone (MCH66C8) from the weakly invasive cell line. We compared the biological activities of invasiveness and angiogenesis of these three cell lines, and using differential screening of mRNA populations, identified several candidate genes that were overexpressed in MCH66, and that may play a role in an invasion-independent metastatic pathway.

Materials and Methods

Cell Line Establishment

To establish immortal cell lines, cells from naturally occurring mammary tumors in C3H mice were minced. After removal of large tissue clumps with nylon mesh the cells were plated in Dulbecco's modified Eagle's medium containing 10% fetal bovine serum. Cultures were maintained at 37°C in a humidified 5% CO_2 atmosphere. By observing lung metastasis at 7 weeks after inoculation of 1×10^7 cells in the fat pads of C3H mice, two metastatic cell

Supported by a Grant-in-Aid for Scientific Research (C) (no. 12670212) from the Ministry of Education, Science, Sports, and Culture, Japan.

Accepted for publication February 22, 2002.

Address reprint requests to Takashi Sugino, Department of Pathology, School of Medicine, Fukushima Medical University, 1 Hikariga-oka, Fukushima City, 960-1295, Japan. E-mail: sugino@fmu.ac.jp.

lines, MCH66 and MCH416, were selected. Clonal sublines of MCH66 were isolated by the limiting dilution technique. After fat pad inoculation of 1×10^7 cells, a nonmetastatic clone (MCH66C8) was selected.

Determination of Doubling Time

For growth-rate determination *in vitro*, 1×10^4 cells were seeded into 12-well tissue-culture plates and the number of cells per well determined every 24 hours for 4 successive days. Growth curves were constructed and used to calculate doubling times.

Growth Properties in Vivo *and Spontaneous Metastasis Assay*

Cells (1×10^7) suspended in 200 μl of serum-free Dulbecco's modified Eagle's medium were inoculated into the fat pads of 6-week-old female C3H/He mice. Tumors were surgically removed every week and growth curves constructed by measuring tumor weight. To assay for spontaneous metastasis, five mice from each surgical group were sacrificed at 2 weeks after surgery and the number of lung colonies counted with a dissecting microscope. In addition, at 5 weeks and at 10 to 13 weeks after fat pad inoculation, animals were sacrificed and metastases in major organs were examined.

Morphological and Immunohistochemical Examination

Tumor tissues and general organs were fixed with 10% formalin for paraffin-embedded sections and/or with 4% paraformaldehyde for frozen sections. Sections were hematoxylin and eosin (H&E)-stained and immunostained using a streptavidin-biotin kit (Nichirei, Tokyo, Japan). Sections were incubated with polyclonal rabbit antibodies to laminin (ICN, Costa Mesa, CA), collagen type IV (Progen, Heidelberg, Germany), or heparin sulfate proteoglycan (Chemicon, Temecula, CA) and with monoclonal rat antibody to mouse CD31 (PharMingen, San Diego, CA).

Assessment of Neovascularization

The neovascular development was assessed not by the number but by the area of blood vessels within a tumor because the neovasculature was constructed of dilated and fused sinusoidal vessels. The H&E-stained sections were used to assess neovascular development in each tumor type. Blood vessel morphometry was evaluated in five low-power fields (×40) for every three tumors of each cell line. The areas of blood vessels and tumor parenchyma exclusive of necrosis were measured per each field using a computerized image analyzer (Image-Pro Plus; Media Cybernetics, Silver Spring, MD). The proportion of total vascular area in each tumor was used as an index of vascularity in each tumor cell line.

Gelatin Zymography and Immunoblotting

Protease activities of MCH66 and MCH416 cells were determined using gelatin zymography. Concentrated cultured media containing 10 μg of protein were electrophoresed in 8% sodium dodecyl sulfate-polyacrylamide gel electrophoresis gels co-polymerized with 1 mg/ml of gelatin. Gels were washed for 30 minutes in 2.5% Triton X-100 and incubated in 50 mmol/L of Tris-HCl, pH 7.6, 1 μmol/L of $ZnCl_2$, and 5 mmol/L of $CaCl_2$ for 48 hours at 37°C. After incubation the gels were stained with Coomassie blue. Equal amounts of protein from conditioned media were analyzed by Western blotting using a polyclonal antibody (2 μg/ml) against human 72-kDa gelatinase (IBL, Fujioka, Japan).

Dorsal Air Sac Assay

The dorsal air sac assay was applied to mice to examine the angiogenesis activities of the three cell lines according to methods described by Itoh and colleagues.[2] Millipore chambers containing 1×10^6 cells were implanted into the dorsal subcutaneous tissues of anesthetized female C3H mice. On day 4, after intravenous injection of India ink, angiogenic responses were assessed using dissecting microscope photographs. Vertical histological sections of the subcutaneous tissues were made and the number of blood vessels counted with a computerized image analyzer (Image-Pro Plus, Media Cybernetics).

cDNA Synthesis

Total RNA was extracted from cultured cells using an RNA extraction kit (Qiagen, Tokyo, Japan). Poly(A)$^+$-enriched RNA was obtained using an oligo (dT) purification kit (Promega, Madison, WI). The SMART PCR cDNA synthesis kit (Clontech, Palo Alto, CA) was used to generate high yields of full-length cDNA.

Semiquantitative Reverse Transcriptase-Polymerase Chain Reaction (RT-PCR) and Southern Hybridization

Semiquantitative mRNA analysis using RT-PCR and Southern blot analysis was performed as described.[3] The optimal number of PCR cycles was determined to be 20 to ensure logarithmic amplification. PCR primers sequences were as follows: pleiotrophin, 5′-GCAATATCAGCAGCAACGTAGAAA-3′ and 5′-TGGCGTCTTTT AATCCAGCATC-3′; midkine, 5′-AGTGTTCGGAGTGGACCTGGGG-3′ and 5′-TC CGTTCAGGCTCCAGGCGA-3′; vascular endothelial growth factor, 5′-CGAGACCCTGGTGGACATCT-3′ and 5′-CACCGCCTCGGCTTGTCAC-3′; angiogenin, 5′-GTTGGAAGAGATGGCGATAAGC-3′ and 5′-GACTGACTCTTAA TGGCTTTTGAGAC-3′; platelet-derived growth factor-A, 5′-CGGTCATTTA CGAGATACCT-3′ and 5′-TTTTGTTTTCGCTCTCTGTG-3′; platelet-derived growth factor-B, 5′-GCGACC ACTCCATCCGCTCCTTTG-3′ and 5′-CCGAGCTTGAGGCGTCTTGGCT-3′; basic fibroblast growth

factor, 5′-AGCGGCATCACCTCGCTTCC-3′ and 5′-TGGA AGAAACAGTATGGCCTTCTGTCC-3′; hepatocyte growth factor, 5′-TACA GGGGAACCAGCAATACCA-3′ and 5′-TCAAACTAACCATCCACCCTACTGT-3′; G3PDH, 5′-TTCATTGACCTCAACTACATG-3′ and 5′-GTGGCAGT-GATGGCATGG AC-3′. PCR amplification products were analyzed by Southern-blotting using alkaline-phosphatase-labeled DNA internal oligonucleotides made using Direct Labeling and Detection Systems (Amersham Pharmacia Biotech, Tokyo, Japan).

Suppression Subtractive Hybridization (SSH)

MCH66 cDNA was subtracted against cDNA from MCH416 or MCH66C8 cell lines using the PCR-Select cDNA Subtraction kit (Clontech) according to the manufacturer's protocols. Forward SSH (subtraction of MCH416 or MCH66C8 drivers from MCH66 tester) and reverse SSH (subtraction of tester from drivers) were performed and SSH-PCR products directly ligated into the pGEM T-easy plasmid vector and transfected into JM109 competent cells (Promega). Plasmids containing cloned sequences from the subtracted libraries were identified using the PCR-Select Differential Screening protocol (Clontech). cDNA fragments consistently expressed at higher levels in MCH66 compared to MCH66C8 and MCH416 were sequenced using the Dye Terminator Cycle Sequencing Kit and automated fluorescent DNA sequencer (Amersham Pharmacia Biotech). DNA database searches were performed using the FASTA program and the NCBI DNA Data Bank database.

Virtual Northern Blot Analysis

To confirm the differential expression of the subtracted MCH66 cDNAs, virtual Northern blot analysis was performed. cDNA from all three cell lines (0.2 μg per lane) were electrophoresed, transferred onto nylon membranes, and hybridized with each of the subtracted cDNA probes labeled with alkaline-phosphatase (Amersham Pharmacia Biotech). A mouse G3PDH probe was used as a control. The autoradiograms were analyzed on a densitometer with a computerized image analyzer (Image-Pro Plus).

Results

Establishment of Cell Lines and Growth Properties

Two cell lines were established from spontaneous murine mammary tumors, MCH66 as a noninvasive but metastatic model and MCH416 as an invasive and metastatic model. To facilitate comparative analyses of biological activities and gene expression, we also isolated a non-metastatic clone, MCH66C8, from the MCH66 cell line.

Phase-contrast microscopy showed that MCH66, MCH66C8, and MCH416 cells all demonstrated a polygonal morphology typical of epithelial cells. Although

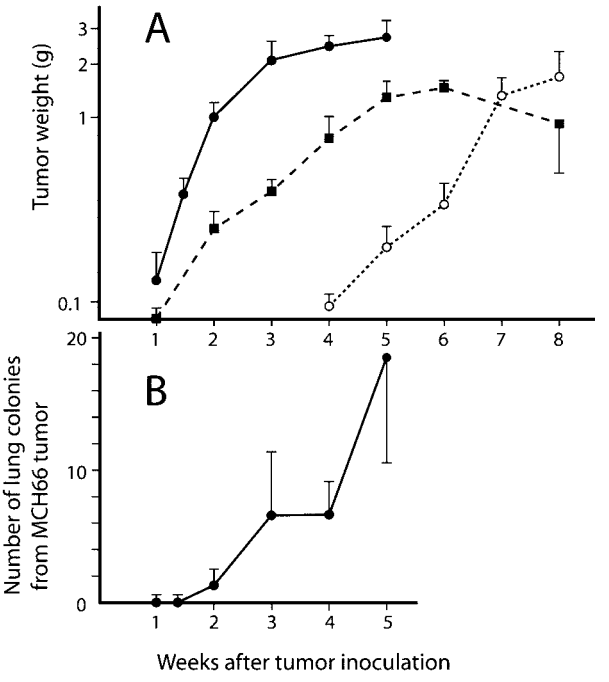

Figure 1. *In vivo* growth properties and generation of pulmonary metastasis. **A:** Tumor growth curves for the subcutaneously inoculated cell lines. **Filled circle**, MCH66; **filled square**, MCH66C8; **open circle**, MCH416. Each point represents the mean ± SEM tumor weight. **B:** Time course of the number of lung metastatic colonies from MCH66 tumors. No colonies were detected in MCH416- or MCH66C8-inoculated mice until 8 weeks after inoculation.

there were no significant differences observed in the *in vitro* doubling times of the MCH66 (14.4 hours) and MCH416 (12.0 hours) cell lines, the MCH66C8 clone exhibited a relatively slower growth rate (19.2 hours).

However, there were marked differences in growth rates *in vivo* (Figure 1A). Although MCH66 became detectable at 7 days after orthotopic inoculation and then exhibited logarithmic growth, MCH66C8 growth was markedly retarded. The MCH416 cells exhibited a 4-week latent growth period and overall growth was much slower relative to MCH66.

Metastatic Propensity of the Cell Lines

Time course observations of secondary lung colony deposits demonstrated that lung metastasis started at 2 weeks after inoculation, when primary tumor weight reached ~1.0 g (Figure 1B). However, MCH416 cells did not give rise to lung metastases until 8 weeks after inoculation when primary tumors reached ~2.0 g in weight (data not shown).

The three cell lines showed marked differences in the incidence and distribution of spontaneous metastasis (Table 1). Mice inoculated with MCH66 cells exhibited a high incidence of metastasis, exclusively localized in the lung, even at 10 to 12 weeks when tumor weights had exceeded 10.0 g. By 10 to 14 weeks, when MCH416 tumors had reached a similar size to that of 5-week MCH66 tumors, the tumor cells had spread widely to multiple organs in blood-borne, lymphatic, and transco-

Table 1. Spontaneous Metastases of Cell Lines

	Cell lines			
	MCH66		MCH66C8	MCH416
Weeks after inoculation	5	10 to 12	10 to 14	12 to 13
Tumor weight, g	2.24 ± 1.14	11.9 ± 7.70	1.65 ± 0.98	3.23 ± 1.70
Incidence of metastasis	11/11	8/9	0/6	15/24
Lung	11/11	8/9	0/6	10/24
Ovary	0/11	0/9	0/6	2/24
Kidney	0/11	0/9	0/6	1/24
Lymph node	0/11	0/9	0/6	8/24
Peritoneum	0/11	0/9	0/6	6/24

Metastases in general organs were examined by dissecting microscopy and confirmed by histological sections. Mice inoculated with 1×10^7 MCH66C8 and MCH416 cells were sacrificed when tumors reached equivalent weights to 5-week MCH66 tumors.

elomic pathways. No MCH66C8 metastases were found in any of the organs examined.

Morphological Differences of Primary Tumors

All three cell lines grew in the mammary fat pad as poorly differentiated adenocarcinomas with solid cellular arrangements. However, each cell line xenograft displayed distinct morphological features. The first feature was invasiveness. Although MCH66 and MCH66C8 cells formed well-demarcated tumors with no detectable invasion (Figure 2, A and B), MCH416 tumors invaded the surrounding fat tissue as early as 7 days after inoculation (Figure 2C). Some late-stage tumors penetrated the abdominal wall and entered the peritoneal cavity.

The second feature was stromal morphology. MCH66 tumors formed small tumor cell nests (50 to 200 μm in diameter) at 7 days after inoculation, and were observed to be surrounded by fibrous stroma (Figure 2D). A continuous basement membrane, containing collagen type IV, laminin, and heparan sulfate proteoglycan, was observed between the tumor cell nest and the stroma (Figure 2E). In contrast, MCH66C8 and MCH416 tumors grew as sheets of cells with scanty fibrovascular stroma.

The third feature was vascular architecture. At 7 days after inoculation, MCH66 tumors induced high peripheral vascularization, such that newly formed blood vessels extended around the tumor nests (Figure 2F). As the tumor grew, the blood vessels developed into fused dilated sinusoidal structures and enveloped entire tumor nests, such that the tumor islands appeared to be entirely surrounded with blood (Figure 2G). Endothelialized tumor nests were observed in the veins draining the tumor and in the pulmonary arterioles. Embolized tumor cells grew expansively within the vessels (Figure 2H), and then extravasated to the lung parenchyma. Conversely, MCH66C8 and MCH416 tumors were poorly vascularized and showed none of the features of intravasation apparent in MCH66 tumors.

Tumor Vascularity and the Correlation to Metastasis

To quantify the vascular development stimulated by the inoculated tumors, intratumoral vascular area was measured using an image analyzer. The proportions of vascular areas in MCH66 tumors were significantly higher than those for MCH416 or MCH66C8 tumors, with the difference being most conspicuous at late growth stages (Figure 3A). The differences in vascular areas between

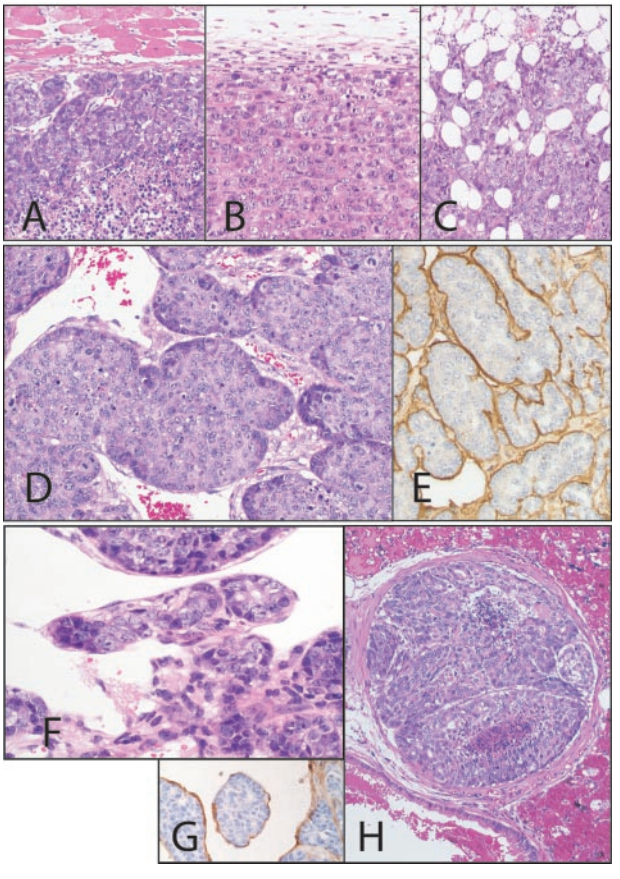

Figure 2. Cell line histology. MCH66 (**A**) and MCH66C8 (**B**) tumors grew expansively, whereas invasive growth of MCH416 (**C**) was evident. **D:** MCH66 tumors at 7 days after inoculation formed small nests surrounded by fibrous stroma. Dilated sinusoidal vessels were observed around the nests. **E:** Immunohistochemistry for laminin shows continuous basement membrane around the MCH66 tumor nests. **F:** MCH66 tumors at 21 days after inoculation. Tumor nest was involved in the developed sinusoidal vessels. **G:** Tumor nest in the blood was surrounded by a vascular endothelial layer that immunostained with anti-CD31 antibody. **H:** Intravascular MCH66 tumor growth subsequent to embolization in the pulmonary arteriole. For laminin and CD31 immunohistochemistry, counterstain is hematoxylin. All others are H&E. Original magnifications: ×100 (**A–C**); ×200 (**D–H**).

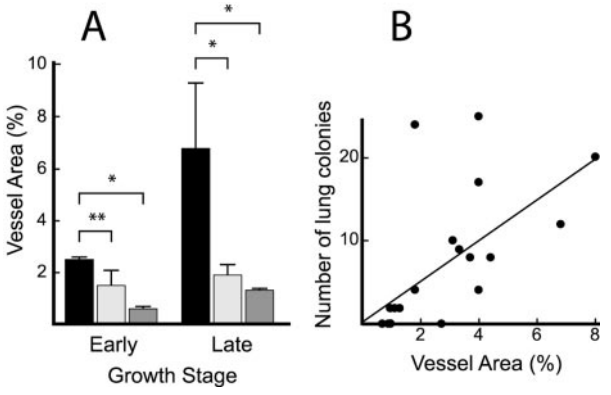

Figure 3. Intratumoral vascularity. **A:** The proportion of vascular area within tumors at an early growth stage (days 12 to 14 of MCH66 and MCH66C8, and day 35 of MCH416) and at a late growth stage (day 35 of MCH66 and days 56 to 70 of MCH416). **Filled square**, MCH66; **light gray square**, MCH66C8; **dark gray square**, MCH416. Results are means ± SEM, $n = 15$ microscopic fields for each group. *, $P < 0.01$; **, $P < 0.05$. **B:** Correlation between the number of pulmonary metastatic colonies in mice inoculated with MCH66 and the proportion of vessel area in the tumors. $P = 0.017$.

the three cell line xenografts seemed to be dependent on the development of sinusoidal vessels.

Among individual MCH66 tumors, we observed a positive correlation between intratumoral vascular area and the number of lung metastatic colonies (Figure 3B). This is in line with the histological findings, indicating that the development of sinusoidal vessels may contribute to the pulmonary metastasis of MCH66 tumors.

Gelatinase Activity

To analyze the gelatinase activity of MCH66 cells we performed gelatin zymography. Weaker gelatinolytic activities of matrix metalloproteinases-2 and -9 were observed in MCH66 cells, relative to that of MCH416 cells (Figure 4A), correlating with the invasive properties of the two cell lines. Immunoblot analysis also detected no MMP-2 protein band present in MCH66-conditioned media (Figure 4B).

Angiogenic Activity

We examined the angiogenic activity of the three cell lines using the dorsal air sac assay. Although MCH66 cells induced numerous neomicrovessels, much less angiogenic activity was stimulated by either MCH416 or MCH66C8 cells (Figure 5A). Image analysis of histological sections also demonstrated a significantly higher angiogenic activity of MCH66 cells relative to both MCH416 and MCH66C8 cells (Figure 5B).

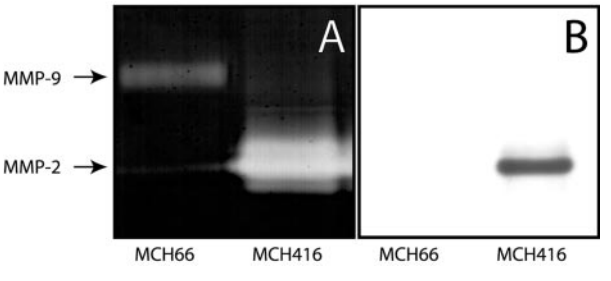

Figure 4. Activities of gelatin degradation and MMP-2 expression. **A:** Gelatin zymography of conditioned media from cultured cells. Molecular weights were calculated using protein standards. **B:** Immunoblot analysis with an MMP-2 antibody confirmed the zymography results.

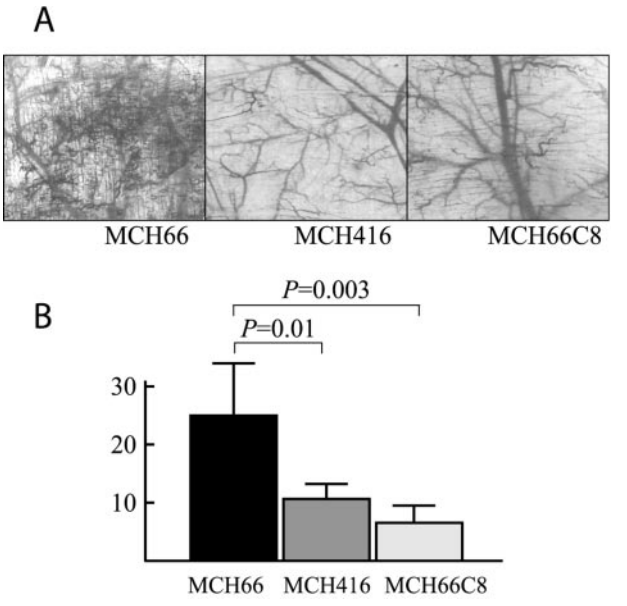

Figure 5. Angiogenesis activities of cell lines using dorsal air sac assay. **A:** Representative views with a dissecting microscopy of the dorsal skin of mice implanted with chambers filled with MCH66, MCH416, or MCH66C8. **B:** The number of vessels per 1-mm width of vertical histological section was estimated using an image analyzer. Results are means ± SEM.

Expression of Angiogenesis Factors

In an attempt to identify the corresponding angiogenesis factors expressed during the increased vascular induction of MCH66, we analyzed specific mRNA expression by semiquantitative RT-PCR and by Southern blot hybridization. Of the angiogenesis factors pleiotrophin, midkine, vascular endothelial growth factor, angiogenin, platelet-derived growth factor-A, and -B, basic fibroblast growth factor, and hepatocyte growth factor, only pleiotrophin was differentially expressed in MCH66 cells (Figure 6A). Expressions of midkine, angiogenin, or platelet-derived growth factor-A or -B were not differential and basic fibroblast growth factor and hepatocyte growth factor were undetectable.

Identification of Differentially Expressed Genes by SSH

SSH was performed to identify genes differentially expressed in the invasion-independent metastatic cell line MCH66. A MCH66 cDNA library was subtracted from either MCH66C8 or MCH416 cDNA libraries and 200 cDNA clones from each subtraction were recovered and maintained by cloning into the TA vector. Reverse Northern analysis identified 82 and 48 MCH66 clones that were differentially expressed relative to MCH66C8 and MCH416, respectively. The 130 cloned sequences con-

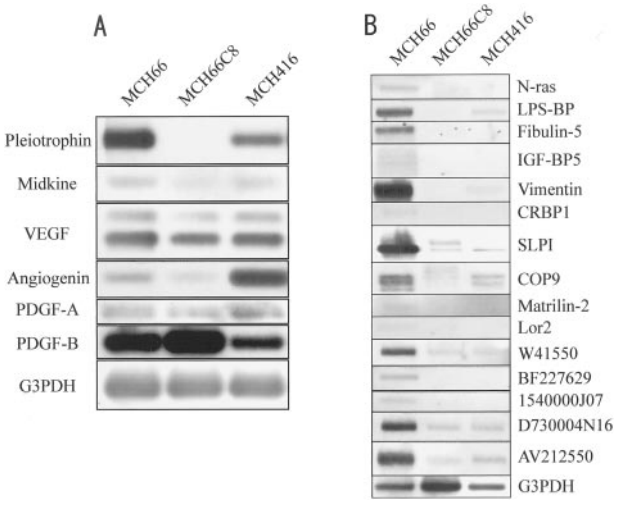

Figure 6. Analysis of differentially expressed MCH66 genes. **A:** Semiquantitative RT-PCR and Southern blot analysis of angiogenesis factors. Basic fibroblast growth factor (bFGF) or hepatocyte growth factor (HGF) expression was not detected in any of the cell lines. VEGF, vascular endothelial growth factor; PDGF, platelet-derived growth factor. **B:** Virtual Northern blot analysis for cDNA clones of known genes from MCH66 libraries subtracted from MCH66C8 and MCH416. LPS-BP, lipopolysaccharide-binding protein; IGFb-BP5, insulin-like growth factor-binding protein-5; CRBP1, cellular retinol binding protein-1; SLPI, secretory leukocyte protease inhibitor.

sisted of 66 unique transcripts and of these, 44 showed homology to known genes, according to searches of available public databases. Virtual Northern analysis identified 15 sequences (10 previously published and 5 expressed sequence tags) that were consistently expressed at higher levels (≥2.0-fold) in MCH66 cells relative to both MCH66C8 and MCH416 cells (Figure 6B and Table 2).

Table 2. List of Differentially Expressed Genes in MCH66

Accession code	Identities	Fold expression to*	
		MCH66C8	MCH416
NM010937	N-ras	7500	1000
NM008489	LPS-BP	2400	7.6
NM011812	Fibulin	240	45
L12447	IGF-BP5	110	18
NM011701	Vimentin	90	15
NM011254	CRBP1	44	6.3
NM011414	SLPI	33	25
NM012004	COP9	26	4.5
U69262	Matrilin-2	20	2.0
NM013586	Lor2	13	17
ESTs			
W41550		466	21
BF227629		273	109
1540000J07		116	13
D730004N16		61	7.7
AV212550		13	6.4

LPS-BP, lipopolysaccharide-binding protein; IGFb-BP5, insulin-like growth factor-binding protein-5; CRBP1, cellular retinol binding protein-1; SLPI, secretory leukocyte protease inhibitor.

*Fold expression levels in MCH66 relative to MCH66C8 and MCH416, respectively, were normalized for G3PDH expressions.

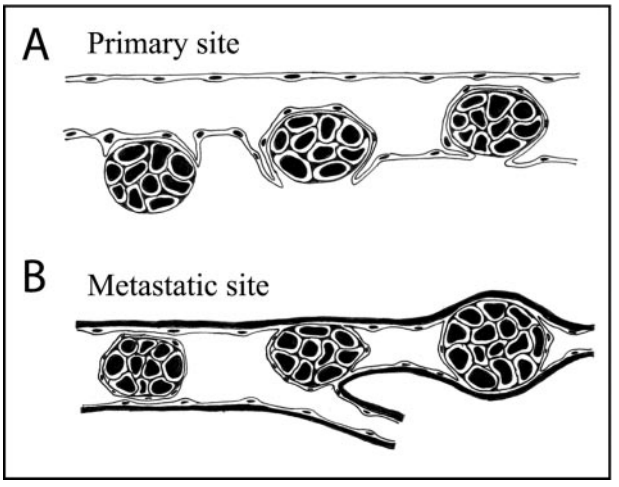

Figure 7. Schematic showing the process of blood-borne metastasis of MCH66 tumors. **A:** Intravasation of a tumor nest enveloped by vascular endothelial cells. **B:** A tumor embolus, conserving its tissue organization and endothelial covering, is mechanically arrested in an arteriole and then intravascularly proliferates. During this metastatic process, the tumor cells do not pass through vascular walls.

Discussion

The sequential process of MCH66 metastasis is schematically illustrated (Figure 7). At the primary site, MCH66 cells intravasate into the newly formed blood vessels that envelop the tumor nests (Figure 7A). In the target organ, the tumor nests realize their metastatic potential by mechanical embolization and intravascular proliferation in the pulmonary arteriole (Figure 7B).

Our findings using this model suggest a metastatic pathway that differs from the currently held concept of metastasis in a number of ways. The first important difference is that the active invasion of cancer cells may not be an absolute requirement for metastasis. In the standard model, cancer metastasis is thought to depend on cellular invasiveness via enzymatic degradation of the extracellular matrix and vascular walls, and cell motility leading to migration into the interspace. In our study, the MCH416 cell line was used as a model of the invasion-dependent metastatic pathway, and showed widespread metastasis based on an invasive phenotype. In contrast, the process enabling the dissemination and secondary growth of MCH66 cells did not involve the penetration of tumor cells into the vascular wall, and therefore did not require invasive activity. In fact, the MCH66 cell line exhibited a higher metastatic potential than the invasive and metastatic cell line MCH416, despite having low invasive activity as indicated by the expansive growth *in vivo* and weak gelatin-degrading activity. To our knowledge, this is the first description of a metastatic model that is independent of invasive ability.

Another aspect of metastasis revealed during the study of this model concerns the morphology of the tumor emboli in the circulation. Most experimental studies on metastasis have supposed that tumor emboli are disorganized clumps of cells that have become detached through the loss of intercellular adhesion. However, in our system the tumor cells conserved tissue organization by

maintaining a nested architecture throughout the metastatic process. In line with this finding, several studies have demonstrated that intravenously injected multicellular tumor clusters have higher metastatic efficiencies than single cells.[4–6] The well-organized MCH66 tumor cell emboli presumably have an advantage of survival and proliferation in the blood vessels, and this may be further enhanced by the fact that the tumor cell emboli in the circulation remain covered by a vascular endothelial cell layer. There has been little discussion on whether stromal elements accompany metastatic cancer cells, instead more emphasis has been placed on sole cancer cells moving to, and thriving in target organs. Further studies are required to clarify the fate and role of tumor-accompanying vascular cells, both in the circulation and at the target organ.

The most critical step in the generation of the MCH66 tumor emboli seemed to be intravasation. The finding that vascularity in MCH66 tumors was significantly higher than in MCH416 or MCH66C8 tumors and positively correlated with the number of lung metastatic colonies suggests an important role for sinusoidal development of tumor vasculature in the intravasation process. In a variety of human cancers, intratumoral vascularity is strongly associated with metastasis and patient prognosis.[7–9] However, apart from tumor growth, there has been no definitive explanation for a direct role of increased tumor vascularity in the metastatic process. Our results demonstrate a direct relationship between tumor angiogenesis and intravasation, and suggest that metastasis is dependent not only on vascularity but also on vascular morphology.

Our studies suggest the possibility that two biological activities are involved in the development of the sinusoidal vasculature that envelope the tumor nests. One is angiogenesis activity; the dorsal air sac assay demonstrated higher angiogenic activity in MCH66 tumors than in MCH66C8 or MCH416 tumors. The observed more rapid growth of MCH66 tumors *in vivo* may be because of this activity. Analysis of a panel of known angiogenesis-related factors showed that only pleiotrophin could be regarded as a plausible candidate for this activity. Pleiotrophin is a secreted angiogenesis factor expressed in a variety of tumors,[10] and the ribozyme targeting of pleiotrophin has been shown to reduce the growth, angiogenic activity, and metastasis of human melanoma cells.[11]

Another activity that may be involved in the development of endothelialized tumor emboli in sinusoidal vessels is vascular remodeling. Our time-course observations of MCH66 tumors after inoculation demonstrated the formation of tumor nests surrounded by basement membrane and fibrous stroma before associated vascular spreading, and the consequent vascular development into sinusoidal structures. It is known that extracellular matrix components induce angiogenesis.[12,13] Heparan-sulfate proteoglycan, a basement membrane component, can bind to various heparin-binding growth factors including vascular endothelial growth factor, basic fibroblast growth factor, and pleiotrophin.[14–16] Therefore, in addition to angiogenesis induction, extracellular matrix components assembled around MCH66 tumor nests may also participate in the generation of sinusoidal vessels that allow, or facilitate intravasation. In fact, several molecules that were found to be differentially expressed in MCH66 cells by SSH are related to cell-stromal interaction and extracellular matrix assembly. Fibulin-5 is an epidermal growth factor-like protein expressed in developing arteries and neural crest-derived tissues.[17] Fibulin-5 is a novel vascular ligand for integrin receptors that may play a role in vascular development and remodeling. Matrilin-2 is an oligomeric protein that forms a filamentous network in the extracellular matrices of various tissues, but its functions are yet to be fully determined.[18,19] The *Lor-2* gene encodes a novel lysyl oxidase-related protein thought to be a key enzyme in the control of collagen and elastin maturation.[20] These findings support the hypothesis that extracellular matrix components may promote invasion-independent metastasis.

Our results demonstrate that the metastatic potential of the MCH66 murine tumor model is dependent not on invasiveness, but on tumor angiogenesis. Although this model would not be applicable to the metastasis of all human cancers, microscopical observations of routine surgical specimens do suggest that similar metastatic processes may occur in some types of human cancer. For example, textbooks of pathology describe intravascular tumor emboli of follicular carcinoma of the thyroid that are covered by endothelial cells.[21,22] Further detailed investigations are required to find out if this model also applies to other kinds of human cancer.

The derivation of these mammary tumor cell lines provides a pertinent experimental system for controlled invasion-independent metastasis evaluation and will greatly facilitate the identification of genetic and biochemical differences involved in the cancer metastasis. Manipulation of candidate genes and subsequent analysis of upstream and downstream effects will permit evaluation of important outstanding questions in this field.

References

1. Sugino T, Kawaguchi T, Suzuki T: Sequential process of blood-borne lung metastases of spontaneous mammary carcinoma in C3H mice. Int J Cancer 1993, 55:141–147
2. Itoh T, Tanioka M, Yoshida H, Yoshioka T, Nishimoto H, Itohara S: Reduced angiogenesis and tumor progression in gelatinase A-deficient mice. Cancer Res 1998, 58:1048–1051
3. Mohler KM, Butler LD: Quantitation of cytokine mRNA levels utilizing the reverse transcriptase-polymerase chain reaction following primary antigen-specific sensitization in vivo. I. Verification of linearity, reproducibility and specificity. Mol Immunol 1991, 28:437–447
4. Fidler IJ: The relationship of embolic homogeneity, number, size and viability to the incidence of experimental metastasis. Eur J Cancer 1973, 9:223–227
5. Liotta LA, Saidel GM, Kleinerman J: The significance of hematogenous tumor cell clumps in the metastasis process. Cancer Res 1979, 36:889–894
6. Glaves D: Correlation between circulating cancer cells and incidence of metastasis. Br J Cancer 1983, 48:665–673
7. Weidner N, Semple JP, Welch WR, Folkman J: Tumor angiogenesis and metastasis-correlation in invasive breast carcinoma. N Engl J Med 1991, 324:1–8
8. Macchiarini P, Fontanini G, Hardin MJ, Squartini F, Angeletti CA:

Relation of neovascularisation to metastasis of non-small-cell lung cancer. Lancet 1992, 340:145–146
9. Li VW, Folkerth RD, Watanabe H, Yu C, Rupnick M, Barnes P, Scott RM, Black PM, Sallan SE, Folkman J: Microvessel count and cerebrospinal fluid basic fibroblast growth factor in children with brain tumours. Lancet 1994, 344:82–86
10. Schulte AM, Wellstein A: Pleiotrophin and related molecules. Tumor Angiogenesis. Edited by R Bicknell, CE Lewis, N Ferrara. Oxford, Oxford University Press, 1997, pp 273–289
11. Czubayko F, Riegel AT, Wellstein A: Ribozyme-targeting elucidates a direct role of pleiotrophin in tumor growth. J Biol Chem 1994, 269: 21358–21363
12. Vlodavsky I, Miao HQ, Benezra M, Linder O, Bar-Shavit R, Schmidt A, Peretz T: Involvement of the extracellular matrix, heparan sulphate proteoglycans, and heparan sulphate degrading enzymes in angiogenesis and metastasis. Tumor Angiogenesis. Edited by R Bicknell, CE Lewis, N Ferrara. Oxford, Oxford University Press, 1997, pp 125–140
13. Madri JA: The extracellular matrix and the regulation of angiogenesis. Tumor Angiogenesis and Microcirculation. Edited by EE Voest, PA D'Amore. New York, Marcel Dekker, Inc., 2001, pp 9–28
14. Folkman J, Klagsbrun M, Sasse J, Wadzinski M, Ingber D, Vlodavsky I: A heparin-binding angiogenic protein-basic fibroblast growth factor is stored within basement membrane. Am J Pathol 1988, 130:393–400
15. Park JE, Keller GA, Ferrara N: The vascular endothelial growth factor (VEGF) isoforms: differential deposition into the subepithelial extracellular matrix and bioactivity of extracellular matrix-bound VEGF. Mol Biol Cell 1993, 4:1317–1326
16. Raulo E, Chernousov MA, Carey DJ, Nolo R, Rauvala H: Isolation of a neuronal cell surface receptor of heparin binding growth-associated molecule (HB-GAM). Identification as N-syndecan (syndecan-3). J Biol Chem 1994, 269:12999–13004
17. Nakamura T, Ruiz-Lozano P, Lindner V, Yabe D, Taniwaki M, Furukawa Y, Kobuke K, Tashiro K, Lu Z, Andon NL, Schaub R, Matsumori A, Sasayama S, Chien KR, Honjo T: DANCE, a novel secreted RGD protein expressed in developing, atherosclerotic, and balloon-injured arteries. J Biol Chem 1999, 274:22476–22483
18. Deak F, Piecha D, Bachrati C, Paulsson M, Kiss I: Primary structure and expression of matrilin-2, the closest relative of cartilage matrix protein within the von Willebrand factor type A-like module superfamily. J Biol Chem 1997, 272 9268–9274
19. Piecha D, Muratoglu S, Morgelin M, Hauser N, Studer D, Kiss I, Paulsson M, Deak F: Matrilin-2, a large, oligomeric matrix protein, is expressed by a great variety of cells and forms fibrillar networks. J Biol Chem 1999, 274:13353–13361
20. Jang W, Hua A, Spilson SV, Miller W, Roe BA, Meisler MH: Comparative sequence of human and mouse BAC clones from the mnd2 region of chromosome 2p13. Genome Res 1999, 9:53–61
21. World Health Organization: Histological Typing of Thyroid Tumours, ed 2. Edited by Hedinger Chr, Williams ED, Sobin LH. Berlin, Springer-Verlag, 1998
22. Rosai J, Carcangiu ML, DeLellis RA: Tumors of the thyroid gland. Atlas of Tumor Pathology. Edited by J Rosai, LH Sobin. Washington, DC, Armed Forces Institute of Pathology, 1992, pp 49–63